Organic Photovoltaics: A Technology Overview

Matthew Wright

UNSW AUSTRALIA

Never Stand Still | Faculty of Engineering | School of Photovoltaic and Renewable Energy Engineering

Content

Part 1: Organic Photovoltaics Overview

- Justification for OPV
- Demonstration of OPV deployment
- Current challenges faced

Part 2: OPV research at UNSW

- Buffer layer optimisation
- Ternary blend organic solar cells

Efficiency

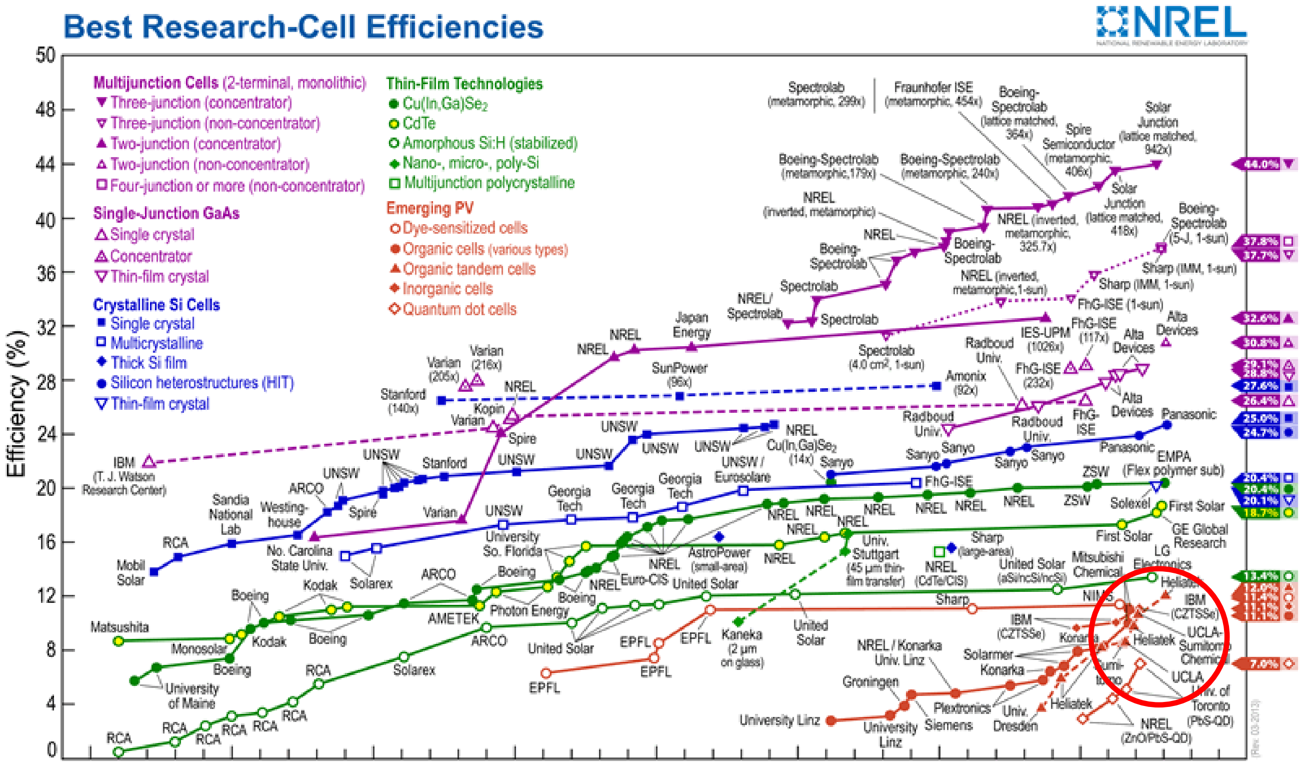

Best Research-Cell Efficiencies
NREL
Efficiency (%)
50
48
44
40
36
32
28
24
20
16
12
8
4
0
1975
1980
1985
1990
1995
2000
2005
2010
2015
Multijunction Cells (2-terminal, monolithic)
Three-junction (concentrator)
Three-junction (non-concentrator)
Two-junction (concentrator)
Two-junction (non-concentrator)
Four-junction or more (non-concentrator)
Single-Junction GaAs
Single crystal
Concentrator
Thin-film crystal
Crystalline Si Cells
Single crystal
Multicrystalline
Thick Si film
Silicon heterostructures (HIT)
Thin-film crystal
Thin-Film Technologies
Cu(In,Ga)Se2
CdTe
Amorphous Si:H (stabilized)
Nano-, micro-, poly-Si
Multijunction polycrystalline
Emerging PV
Dye-sensitized cells
Organic cells (various types)
Organic tandem cells
Inorganic cells
Quantum dot cells
44.0%
37.8%
37.7%
32.6%
30.8%
27.6%
26.4%
25.0%
24.7%
20.4%
20.4%
20.1%
18.7%
13.4%
7.0%

Efficiency

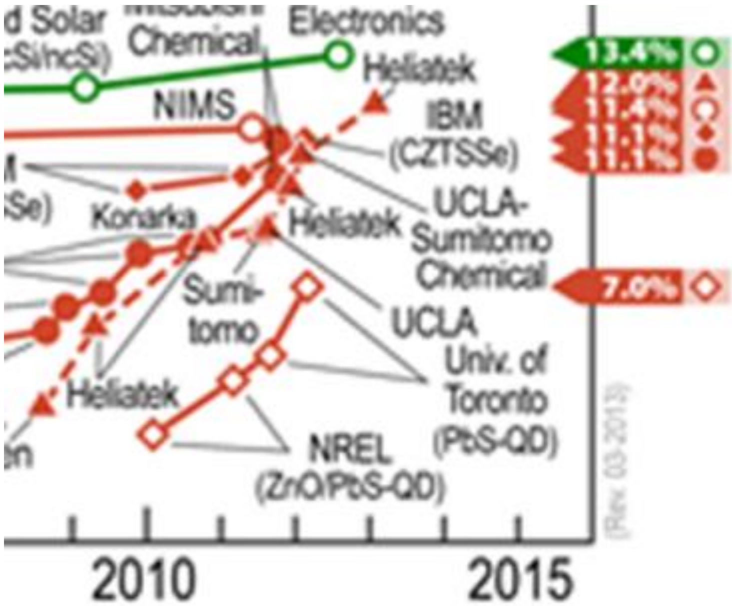

2011: 8.3%

Now: 12%

Efficiency

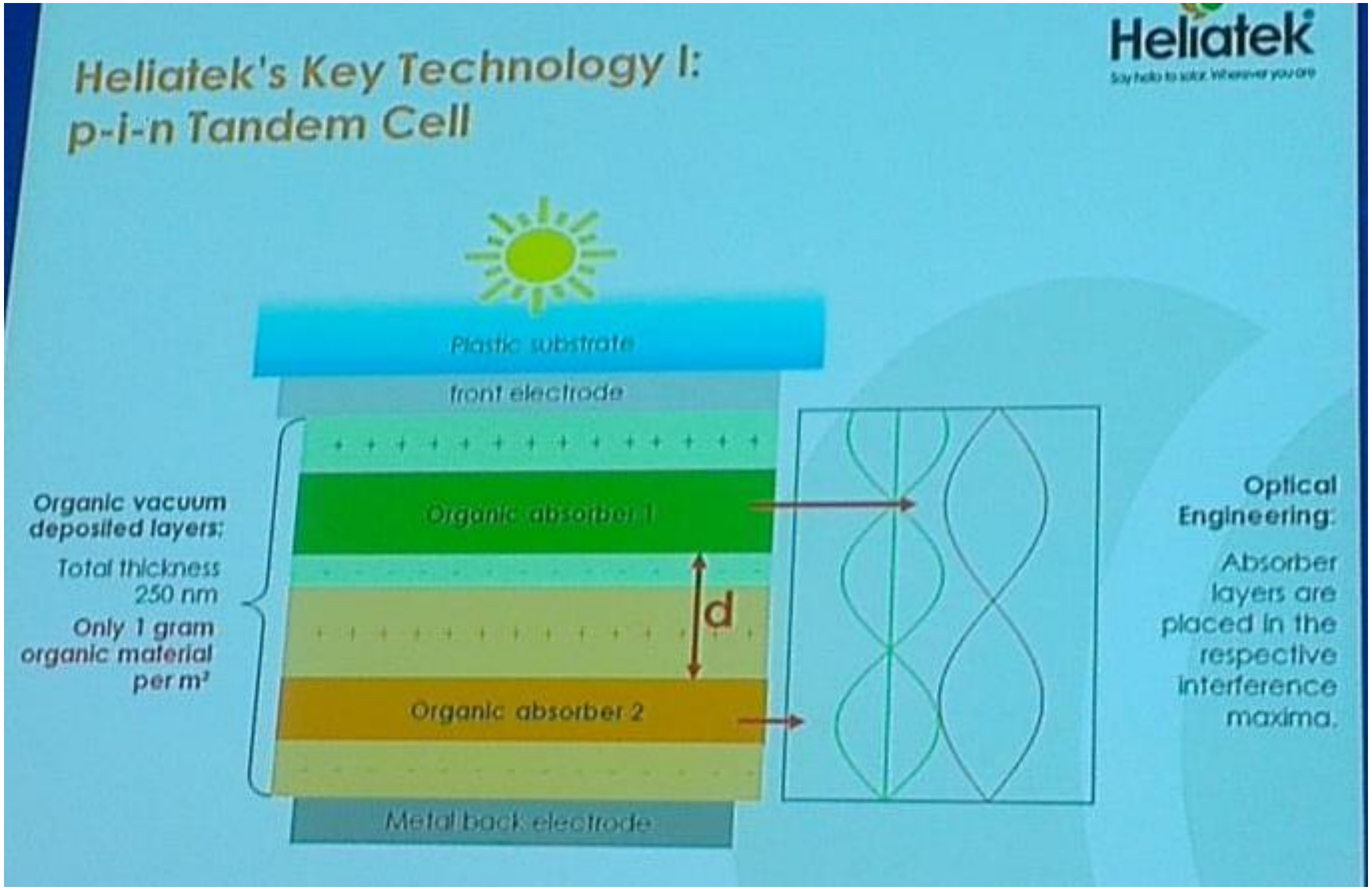

Heliatek's Key Technology I:
p-i-n Tandem Cell
Heliatek
Plastic substrate
front electrode
Organic absorber 1
d
Organic absorber 2
Metal back electrode
Organic vacuum deposited layers:
Total thickness 250 nm
Only 1 gram organic material per m²
Optical Engineering:
Absorber layers are placed in the respective interference maxima.

Efficiency

Published tandem architecture

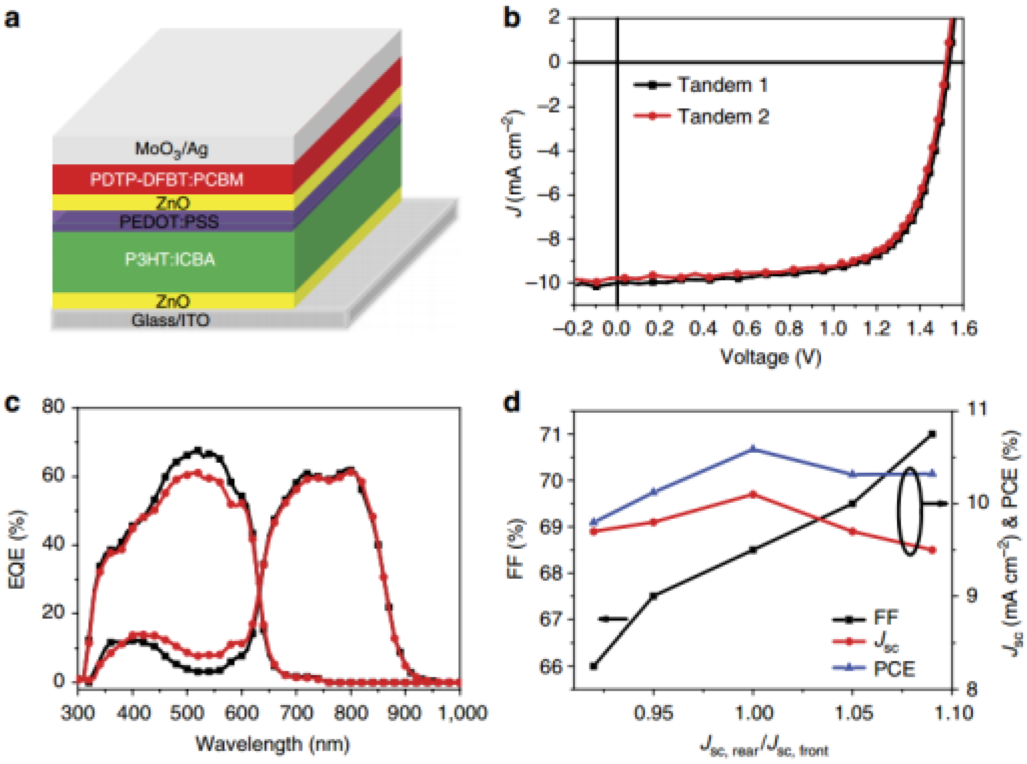

NREL Certified I-V curve

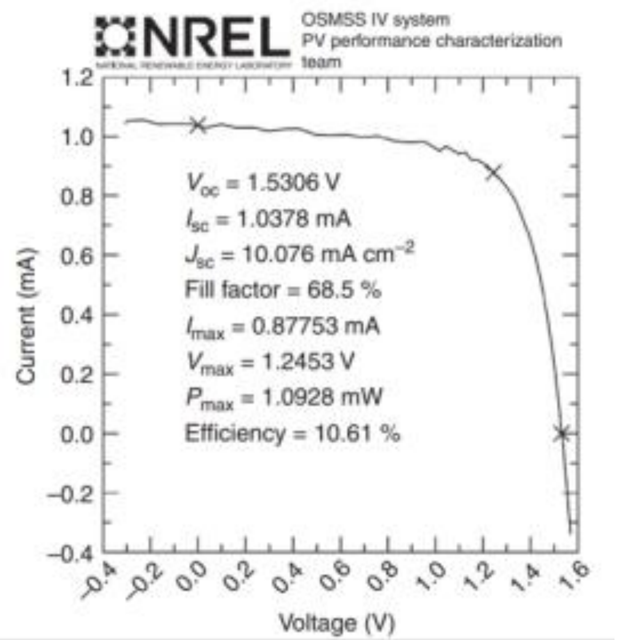

[1]

Efficiency

J_{sc} almost 20 mA/cm^2

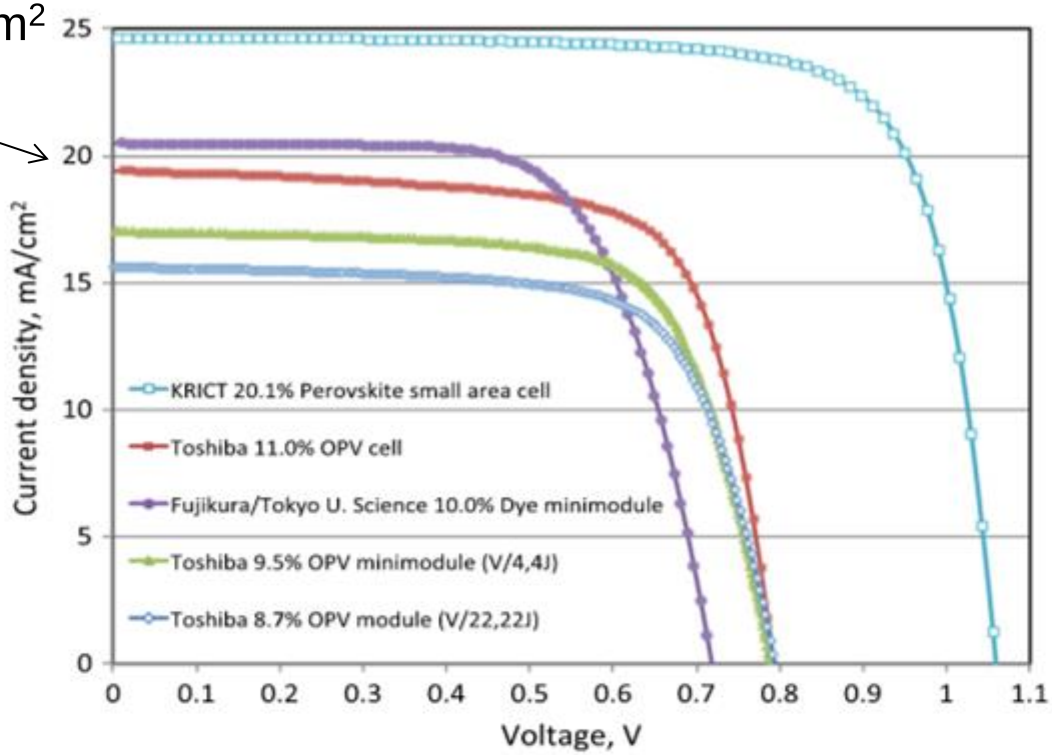

[2]

Justification for OPV

- Solution phase processing for all layers
- High throughput fabrication – scalability
- Low embodied energy
- Flexible and lightweight

Justification for OPV

- Solution phase processing for all layers
- High throughput fabrication – scalability
- Low embodied energy
- Flexible and lightweight

[3]

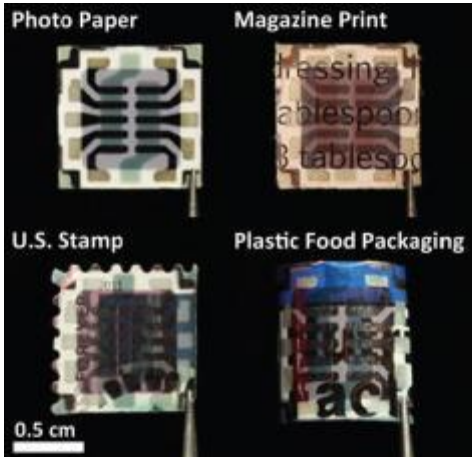

[4]

Life Cycle Analysis for OPV

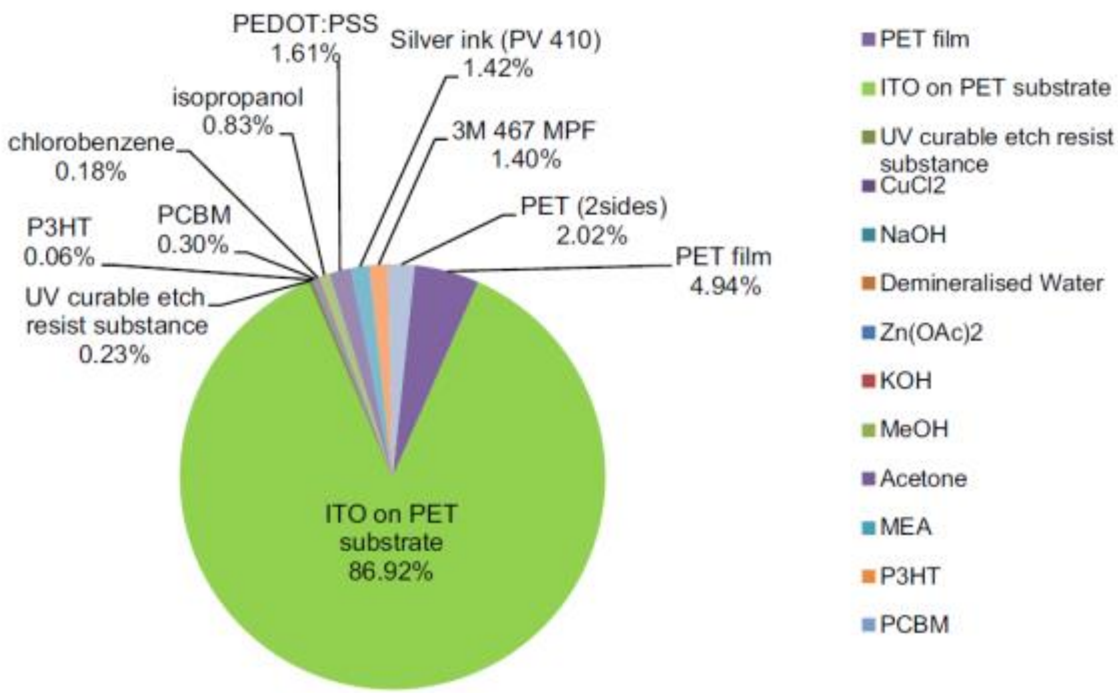

Sputter coated ITO causes unbalanced inventory

Calculated share of embodied energy

[5]

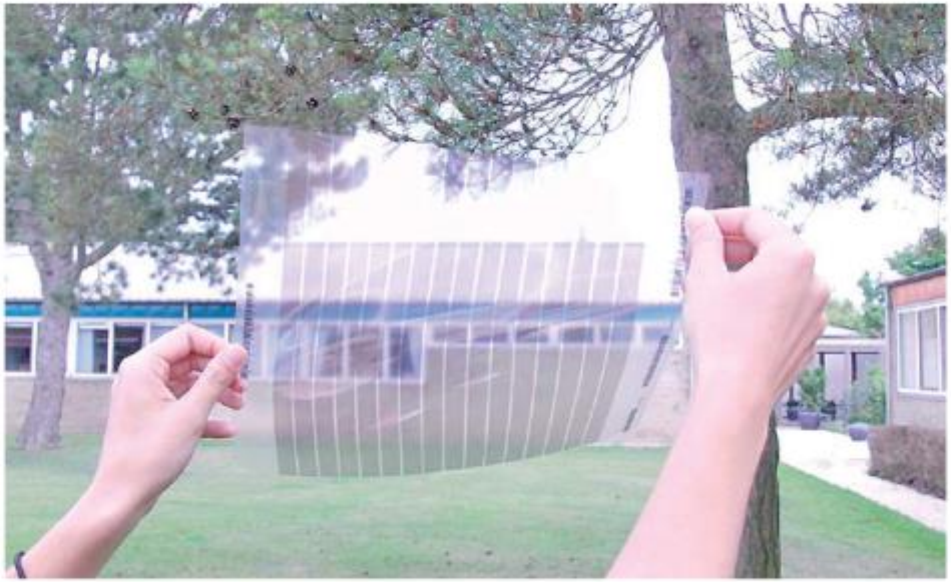

Indium free, thin silver semitransparent front electrode.
Prepared by slot-die coating

[6]

Life Cycle Analysis for OPV

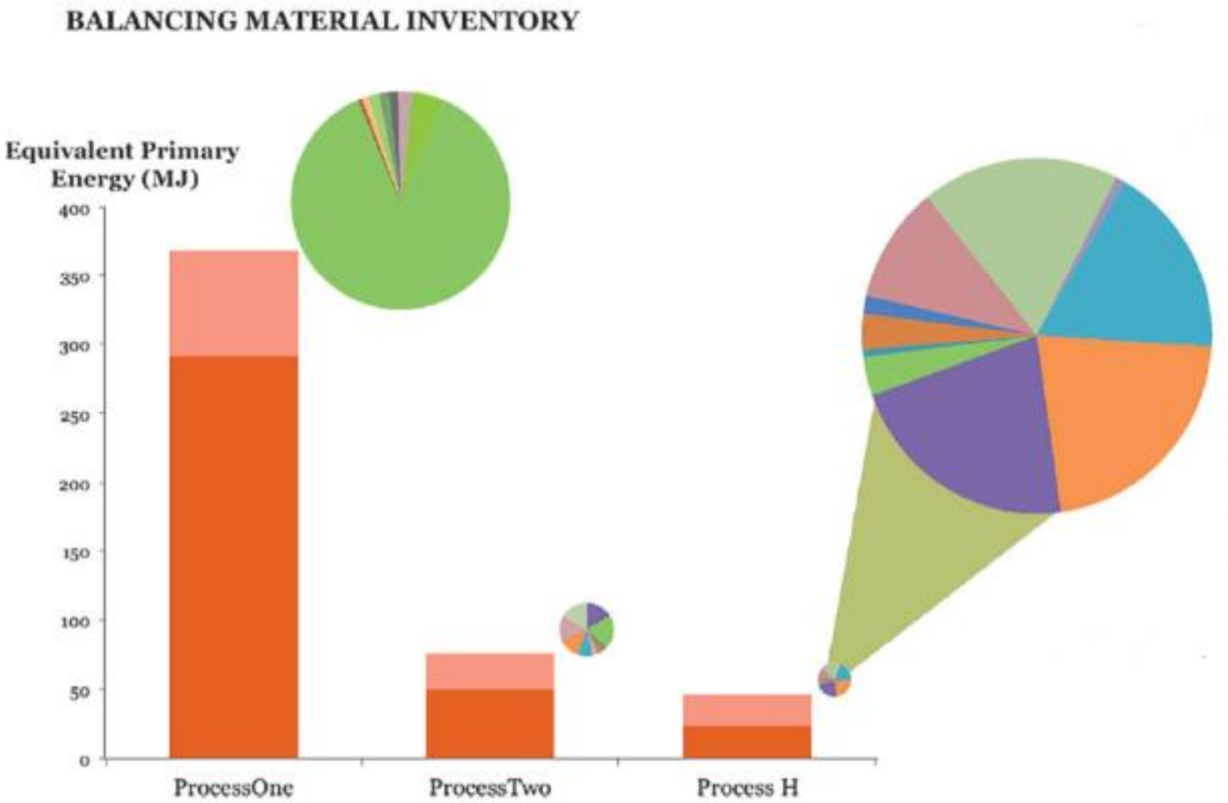

Removing ITO leads to significantly more balanced inventory

[6]

Life Cycle Analysis for OPV

Future work to reduce EPBT:

Feasible assumptions:

- Decreasing layer thickness
- Increasing substrate width
- Increasing geometric fill factor

Challenging assumptions:

- Higher efficiencies
- Increasing lifetimes
- Materials recycling (silver)

[6]

Life Cycle Analysis for OPV

Table 10 EPBT in days *versus* real efficiencies and projections (shaded in grey colour) for Process H in its existing form and when improving following both feasible and challenging developments (shaded in grey colour). Data for ProcessOne are also listed for comparison

Efficiency	0.25%	0.5%	0.7%	1%	2%	3%	5%	10%	15%
ProcessOne	5938.7	2969.4	2120.9	1484.7	742.0	494.8	296.9	148.5	98.9
Process H	1034	517	369	259	129	86	52	26	17
Feasible assumptions	210	105	75	52	26	17	10	5	3
Challenging assumptions	82	41	29	21	10	7	4	2	1

Remove ITO, achieve all “feasible” assumptions, EPBT ~ 1 month

[6]

Deployment of OPV: Solar Park

Processing of OPV modules

Printing of front silver grid

Rotary screen printing of front PEDOT:PSS

Slot-die coating of ZnO

Slot-die coating of P3HT:PCBM

Rotary screen printing of front PEDOT:PSS

Printing of back silver electrode

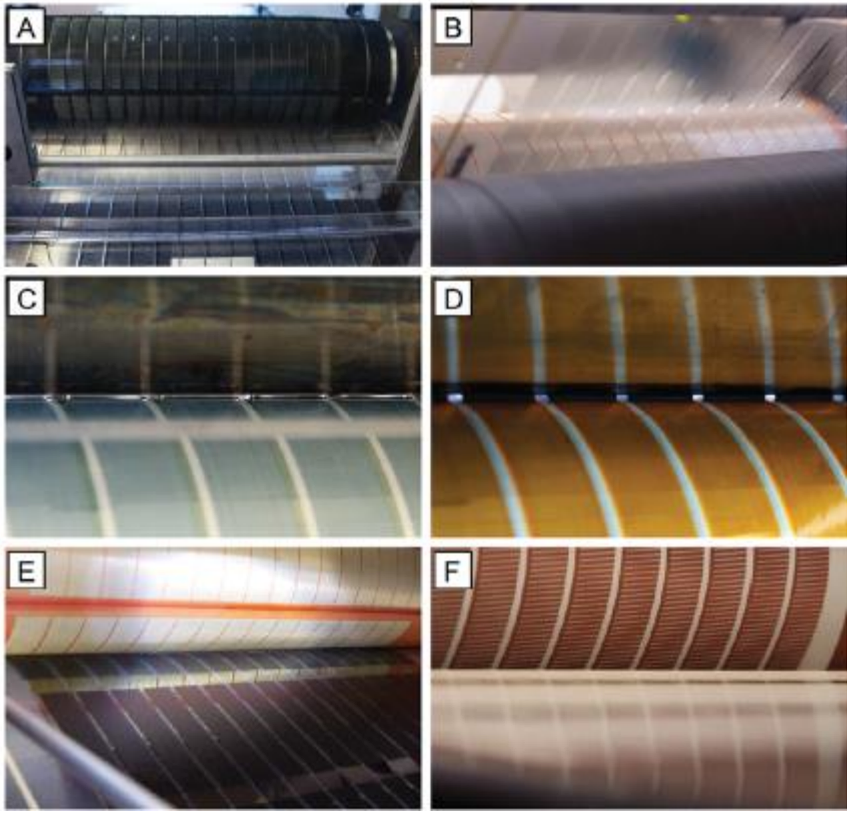

700m foil (147,000 cells) with 100% technical yield

Fabrication speed of 1m / min

[7]

Final product

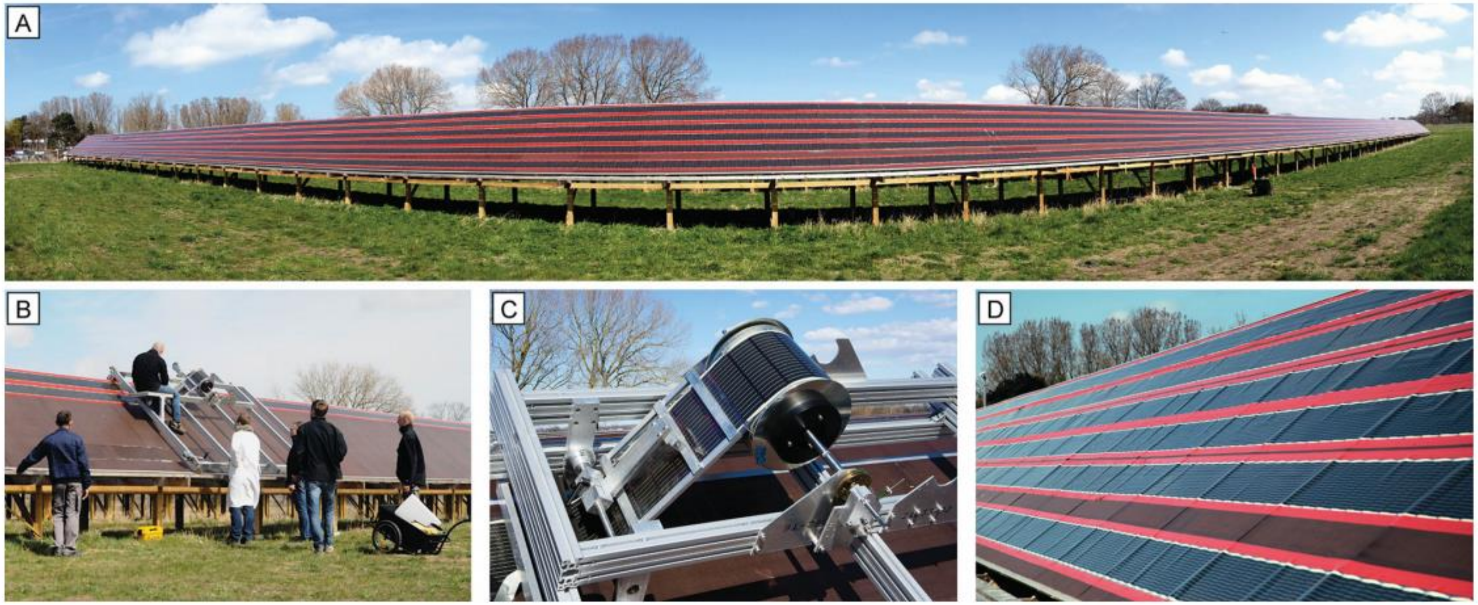

6 lanes x 100m. 305 mm width.

Installation rate 100 m/min. Estimated possible rate of 300 m/min. [7]

Video: Installation of OPV solar park

Deployment of OPV: Solar Park

I-V curve of entire installation

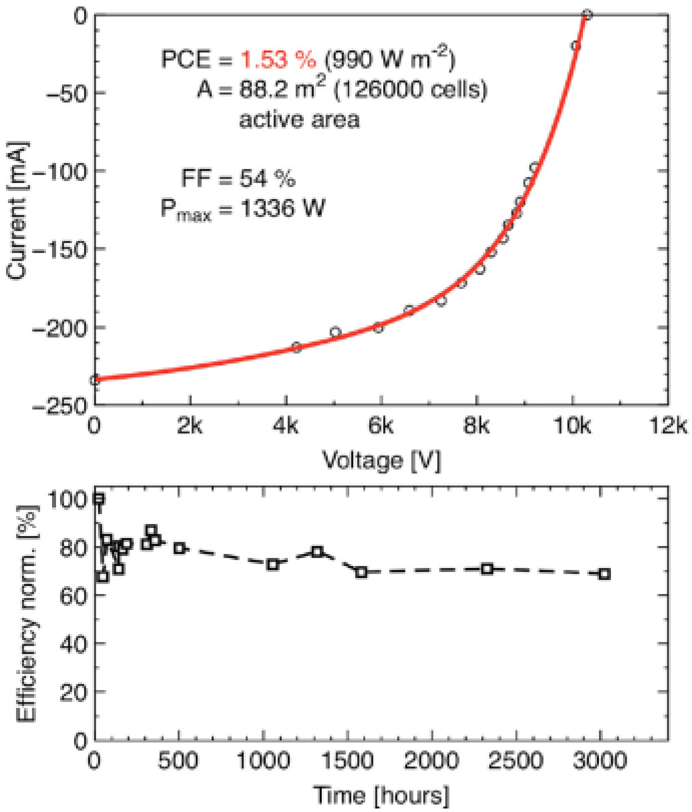

Reduction in performance largely related to FF and V_{oc}

[7]

Deployment of OPV: Solar Park

Energy payback time of components

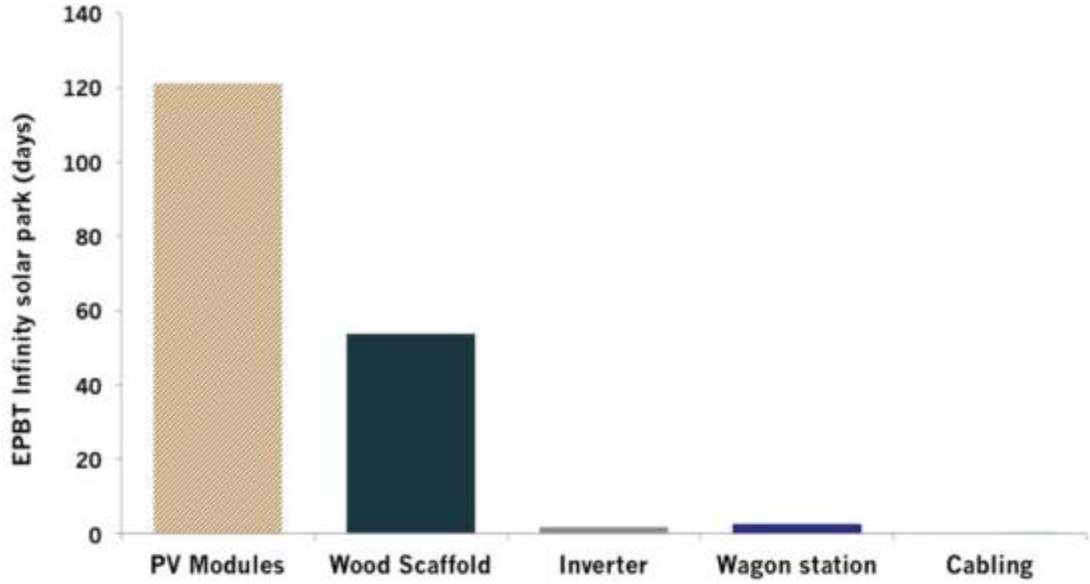

EPBT = 180 (Southern Spain)

Or EPBT = 277 (Denmark)

[7]

Deployment of OPV

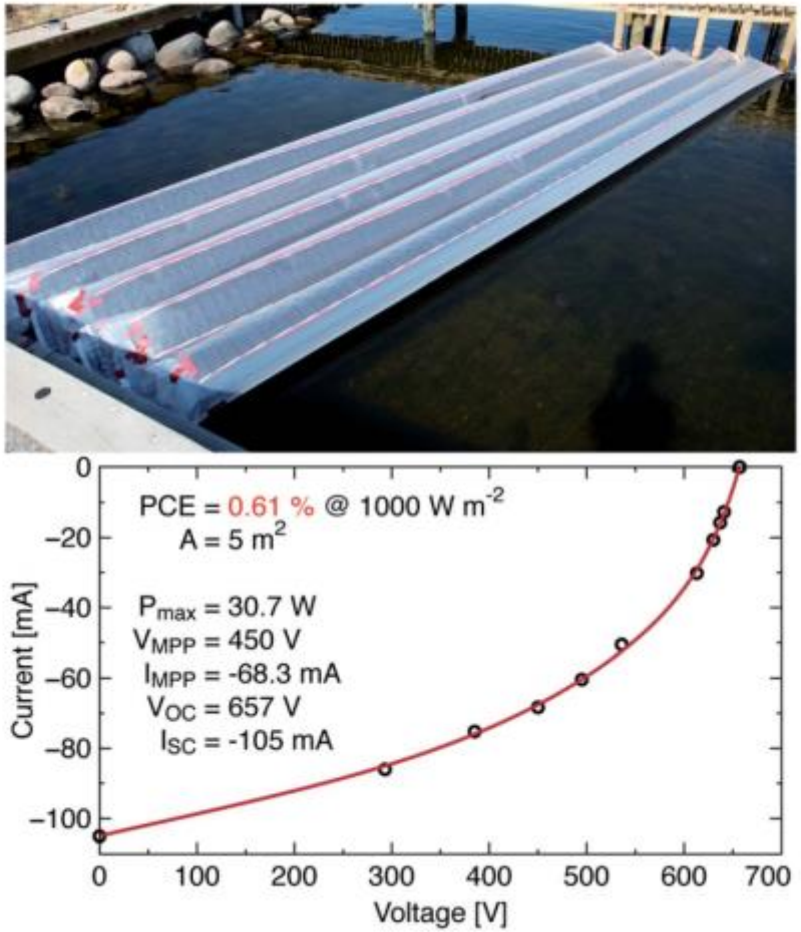

Low density plastic tubes, connected with ropes.

System efficiency of 0.61%.

Due to rough handling during installation

[8]

Deployment of OPV

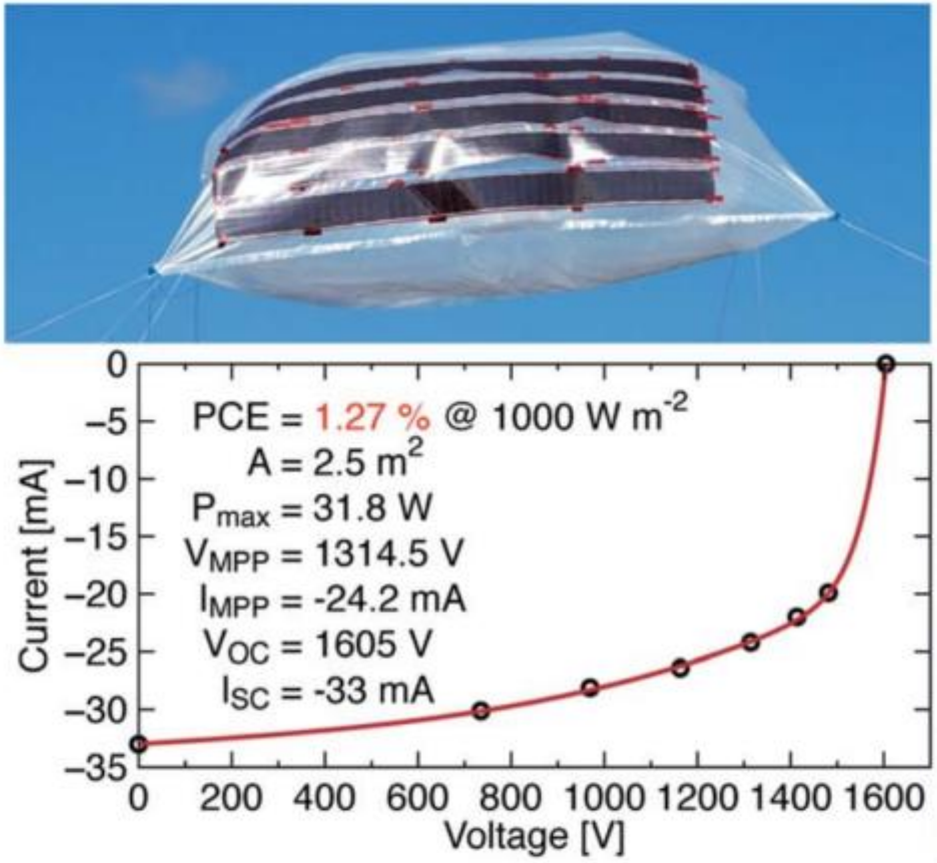

Helium filled balloon,
Dimensions: 4 m x 5 m.

Balloon filled with 16 m^3 of Helium to support 8 kg

Clearly demonstrates unique properties of OPV!

[8]

Deployment of OPV

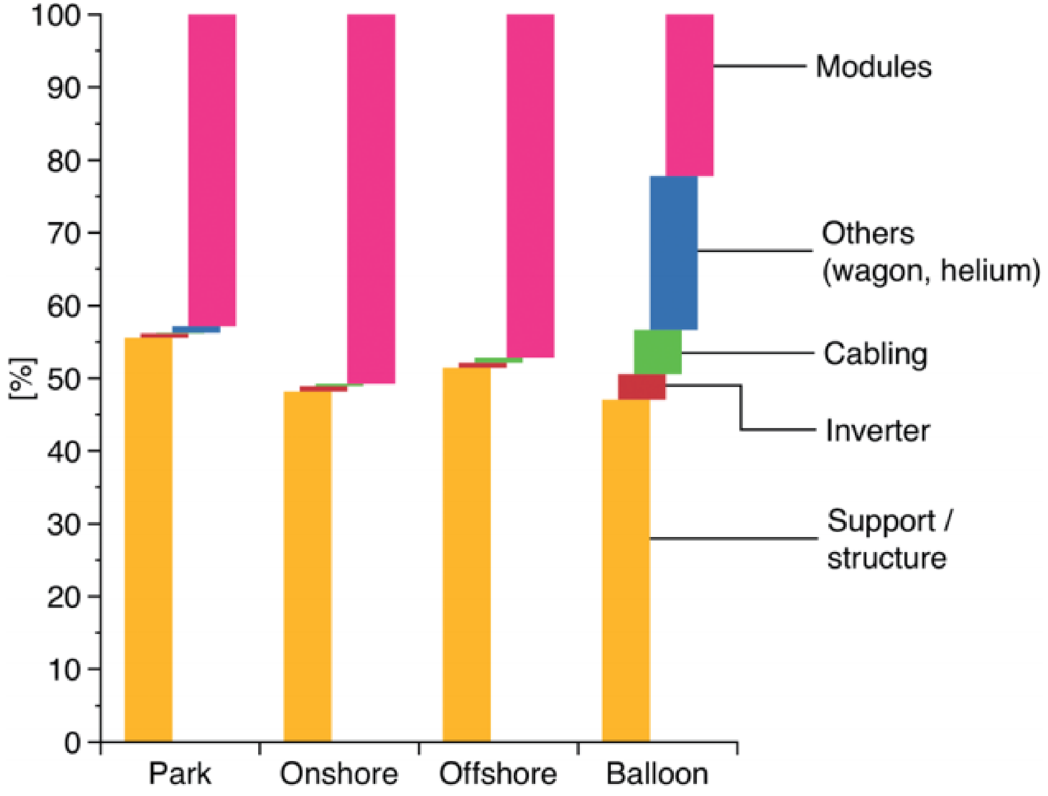

Breakdown of cumulative energy demand required for every component in the BOS for each system

[8]

Solution Processed Perovskite Solar Cells

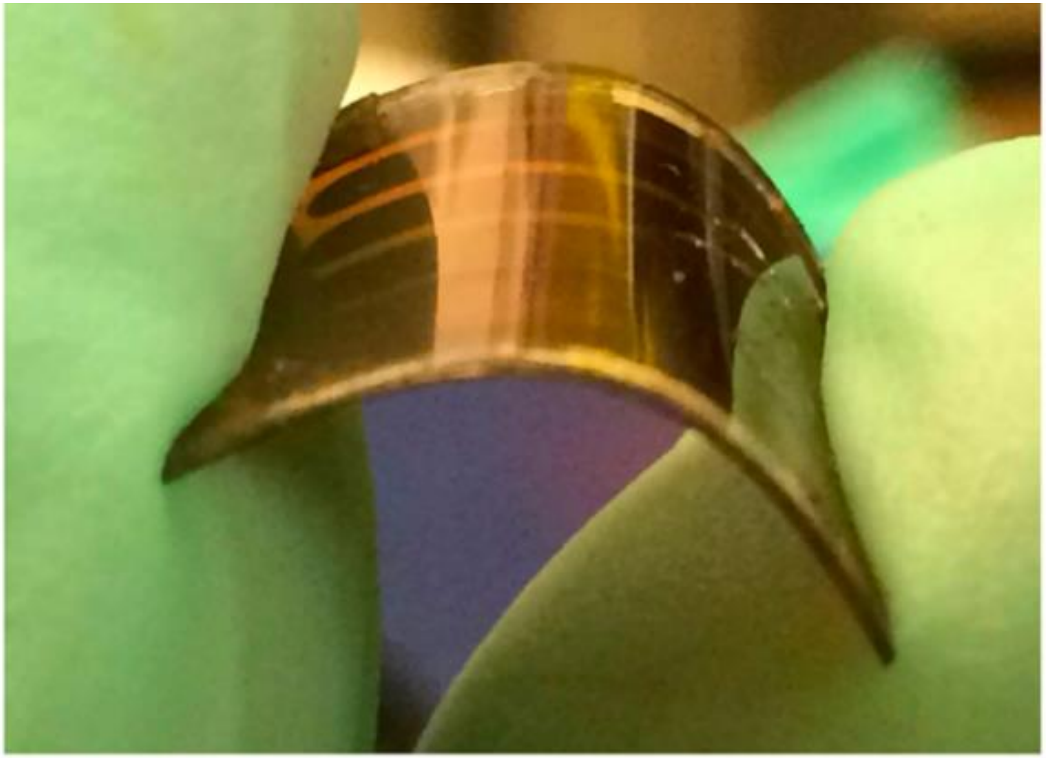

Perovskite solar cell processed on a flexible PET substrate

[9]

Video: Solution based roll coating of a Perovskite layer

Late mail: Investigation of slot-die coating parameters

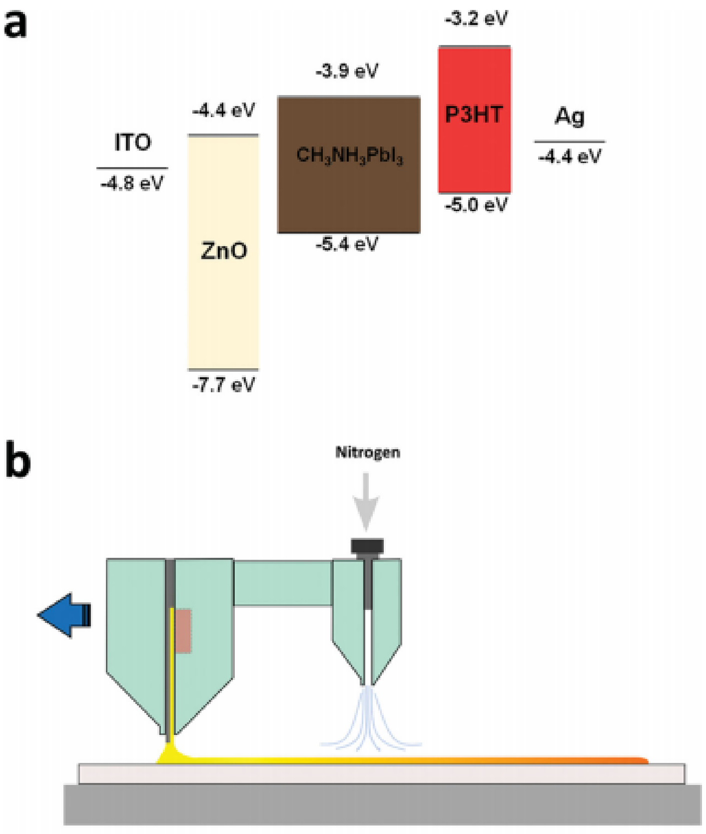

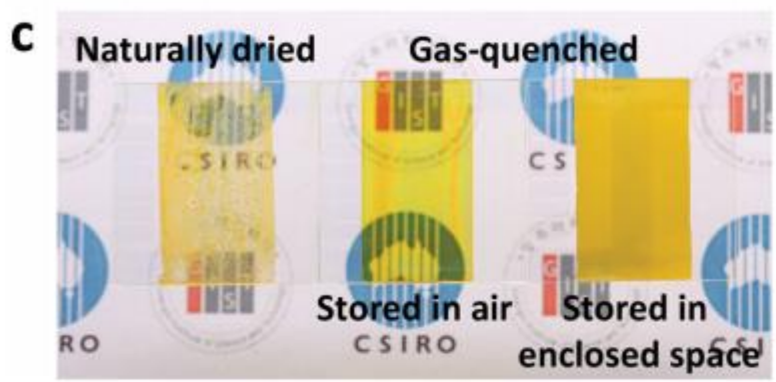

Investigated N_2 gas quenching

[10]

Late mail: Investigation of slot-die coating parameters

Comparison of slot-die / spin coating

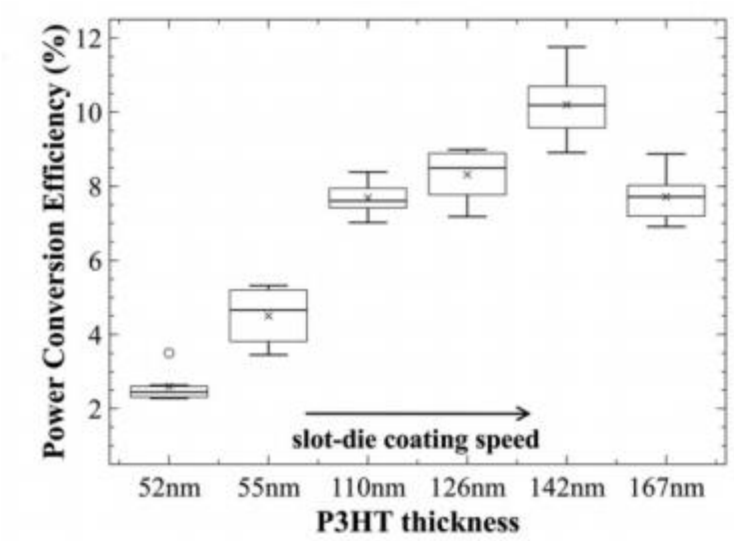

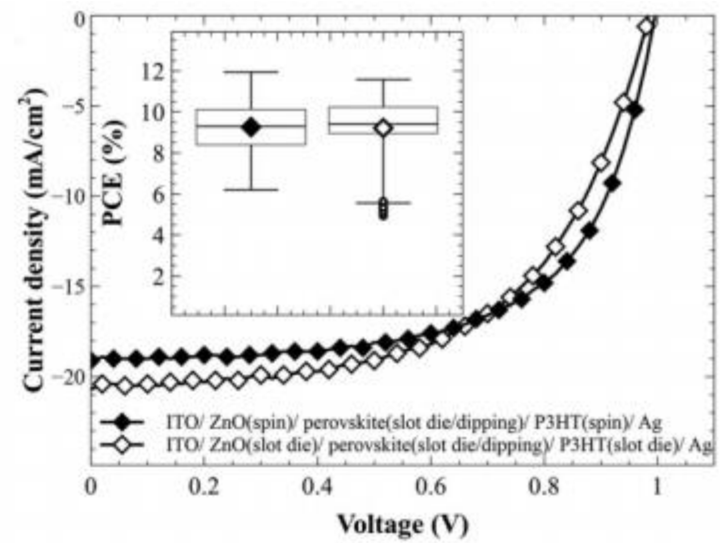

[10]

Challenges faced: Low efficiency

Low efficiency largely related to J_{sc} and FF

Requires synthesis of new polymers which can:

- Have increased spectral breadth
- Improved charge carrier dynamics to increase EQE
- For tandem, require polymers with precisely complementary absorption windows

However, must also be compatible with printing and coating techniques.

Challenges faced: Stability

Significantly lower environmental stability than silicon solar cells.

Mechanisms reducing the stability of OPV devices:

Chemical:

- O_2 / H_2O induced oxidation of organic components
- O_2 / H_2O induced oxidation of electrodes
- Water degradation of PEDOT:PSS (buffer layer)

Mechanical:

- Changes in photoactive morphology
- Delamination at weak interfaces
- Mechanical stresses for flexible substrates, particularly when different layers have different thermal expansion coefficients

Inverted device structure

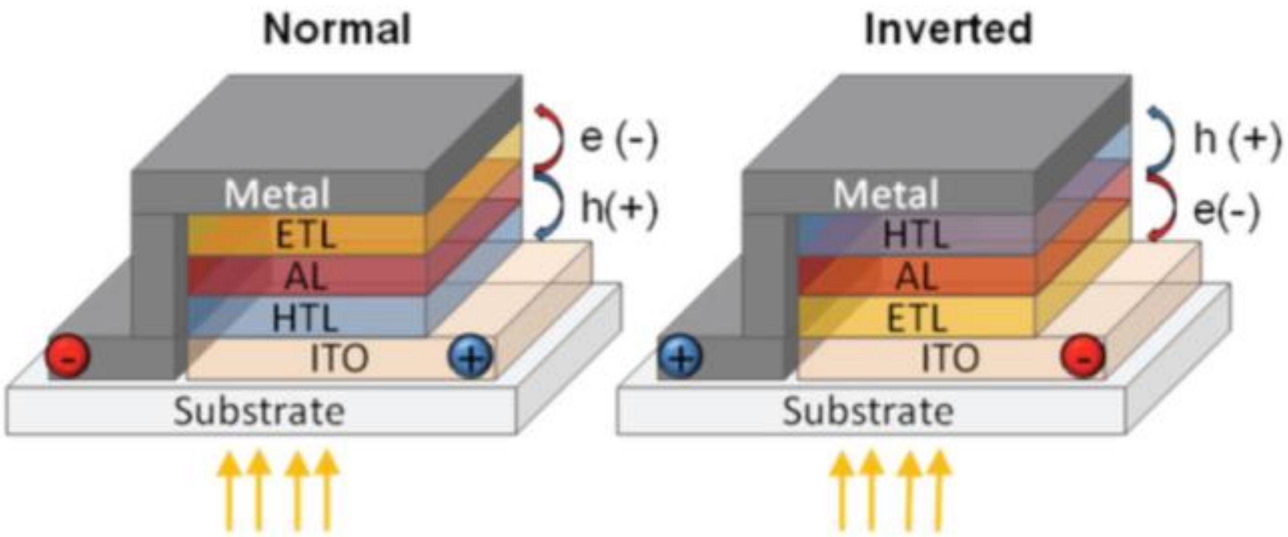

Reverse the direction of charge flow through the device

Silver replaces aluminium as metal electrode

[11]

Challenges faced: Stability

Provides standard protocols established for different testing methods

Undertake and report inter-laboratory 'round robin' tests

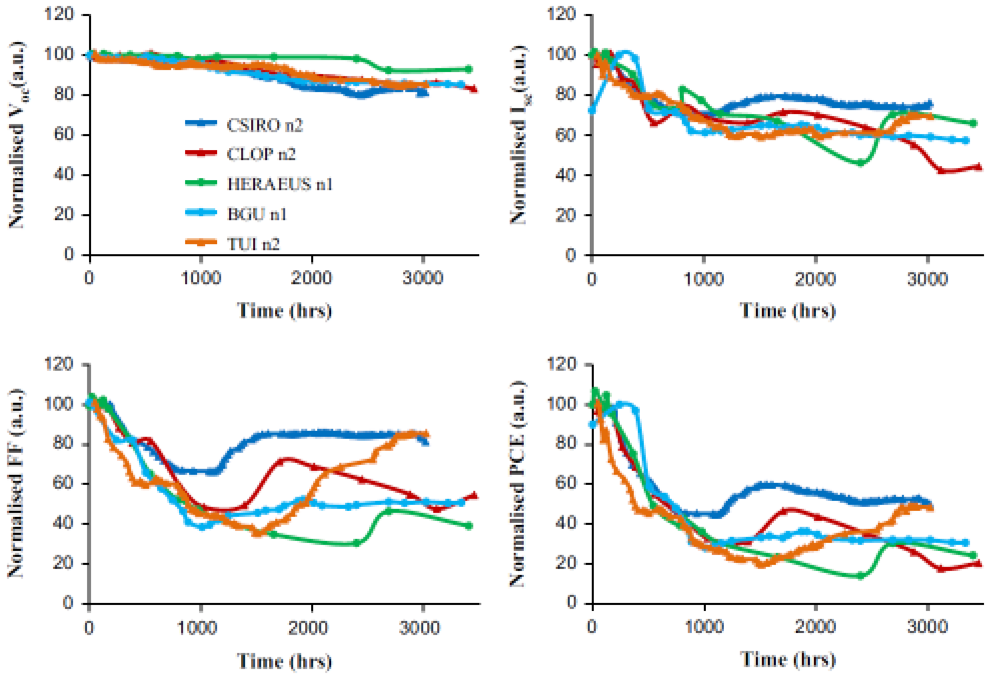

[11]

Photoactive layer →

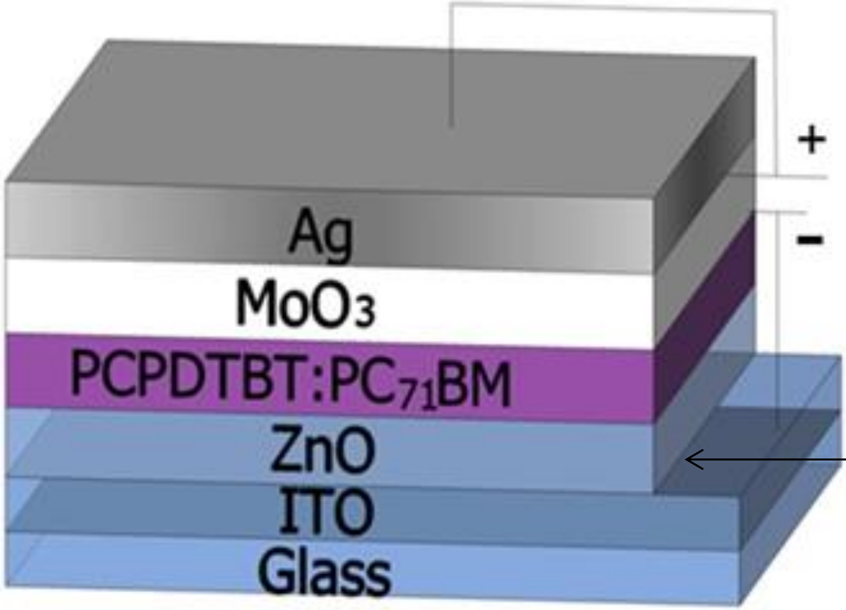

Electron transport layer

ZnO buffer layer

Bare ITO

0.02 g/ml

0.05 g/ml

0.20 g/ml

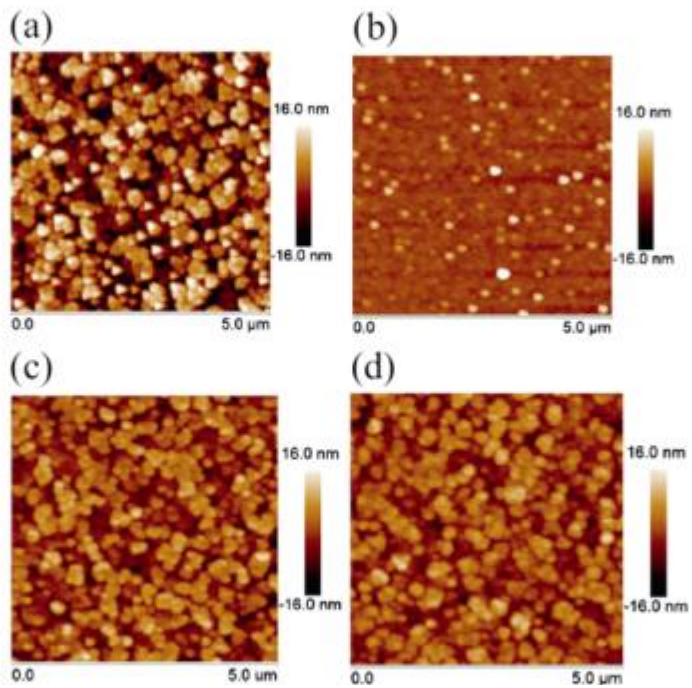

Table 1
PCPDTBT:$PC_{71}BM$ device performance with various zinc acetate concentrations annealed at 250 °C for 60 min. Root mean square (RMS) roughness, ZnO layer thickness, series resistance (R_s), shunt resistance (R_{sh}) and device performance characteristics (V_{oc}, J_{sc}, FF, average PCE and best PCE) are shown.

Concentration (g/ml)	RMS (nm)	Thickness (nm)	V_{oc} (mV)	J_{sc} (mA/cm^2)	FF (%)	R_s ($\Omega \cdot cm^2$)	R_{sh} ($\Omega \cdot cm^2$)	Average PCE (%)	Best PCE (%)
Without ZnO	6.99	0	80 ± 28	4.7 ± 0.5	28.8 ± 3	12.9 ± 2	184 ± 76	0.11	0.15
0.02	2.27	11	121 ± 81	5.8 ± 0.7	29.9 ± 4	13.4 ± 7	237 ± 174	0.22	0.38
0.05	4.39	16	524 ± 14	9.6 ± 0.2	39.6 ± 1	18.0 ± 2	1055 ± 35	1.99	2.13
0.10	4.12	23	569 ± 45	9.8 ± 0.6	38.3 ± 3	17.6 ± 4	1063 ± 20	2.12	2.27
0.20	3.85	29	547 ± 3	9.4 ± 0.1	37.7 ± 1	18.8 ± 1	1010 ± 20	1.94	1.97

[13]

ZnO buffer layer

FTIR spectra

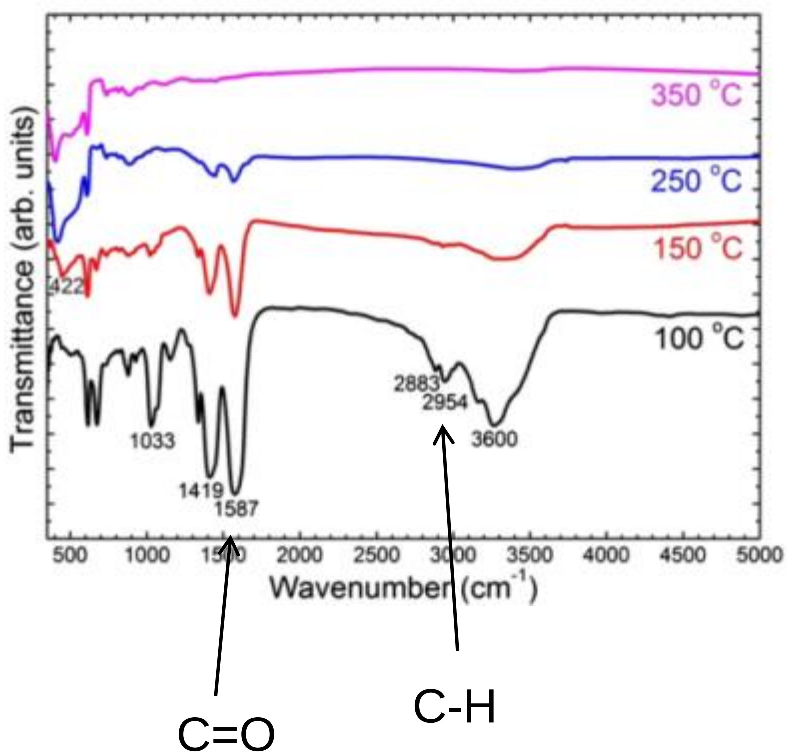

Increasing the annealing temperature improves the conversion of zinc acetate to zinc oxide

Also shown in XPS analysis, reduction in the carbon content of the film

[13]

ZnO buffer layer

SEM images

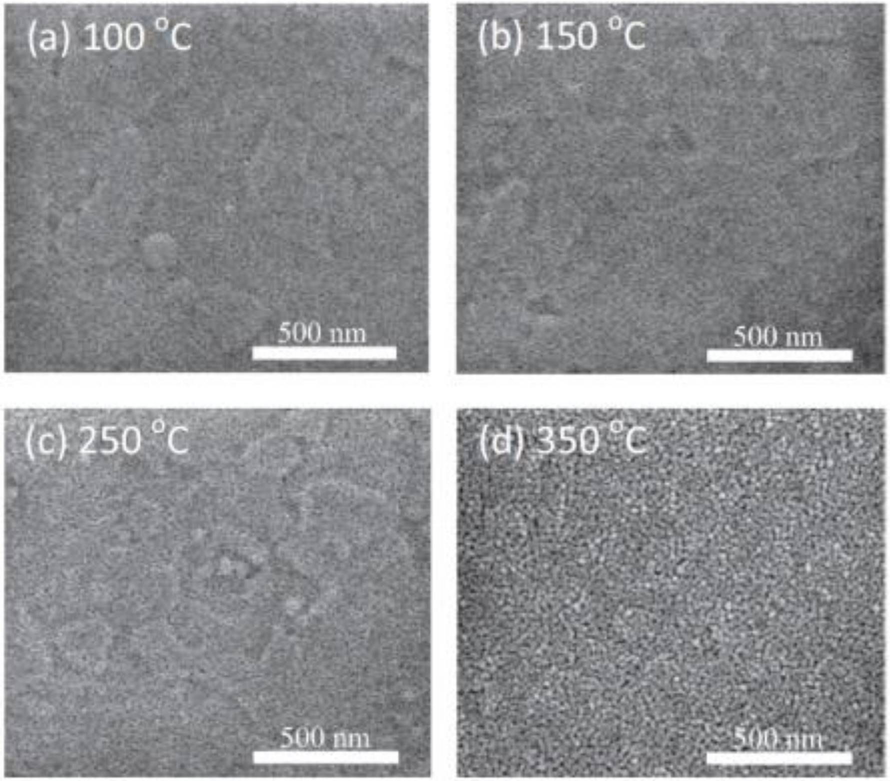

Table 2
PCPDTBT:$PC_{71}BM$ device performance annealed at various ZnO film annealing temperatures for 60 min with a zinc acetate concentration of 0.10 g/ml. Root mean square (RMS) roughness, ZnO thickness, series resistance (R_s), shunt resistance (R_{sh}) and device performance characteristics (V_{oc}, J_{sc}, FF, average PCE and best PCE) are shown.

Annealing temperature (°C)	RMS (nm)	Thickness (nm)	V_{oc} (mV)	J_{sc} (mA/cm^2)	FF (%)	R_s ($\Omega \cdot cm^2$)	R_{sh} ($\Omega \cdot cm^2$)	Average PCE (%)	Best PCE (%)
100	4.75	18	623 ± 12	11.0 ± 0.2	40.1 ± 1	13.7 ± 3	1087 ± 43	2.75	2.81
150	4.58	21	629 ± 42	11.2 ± 1.1	42.5 ± 3	13.3 ± 7	1198 ± 242	3.00	3.43
250	4.12	23	569 ± 45	9.8 ± 0.6	38.3 ± 3	17.6 ± 4	1063 ± 20	2.12	2.27
350	5.00	29	394 ± 44	8.9 ± 0.9	36.2 ± 6	21.0 ± 8	768 ± 119	1.26	1.37

[13]

Ternary blend organic solar cells

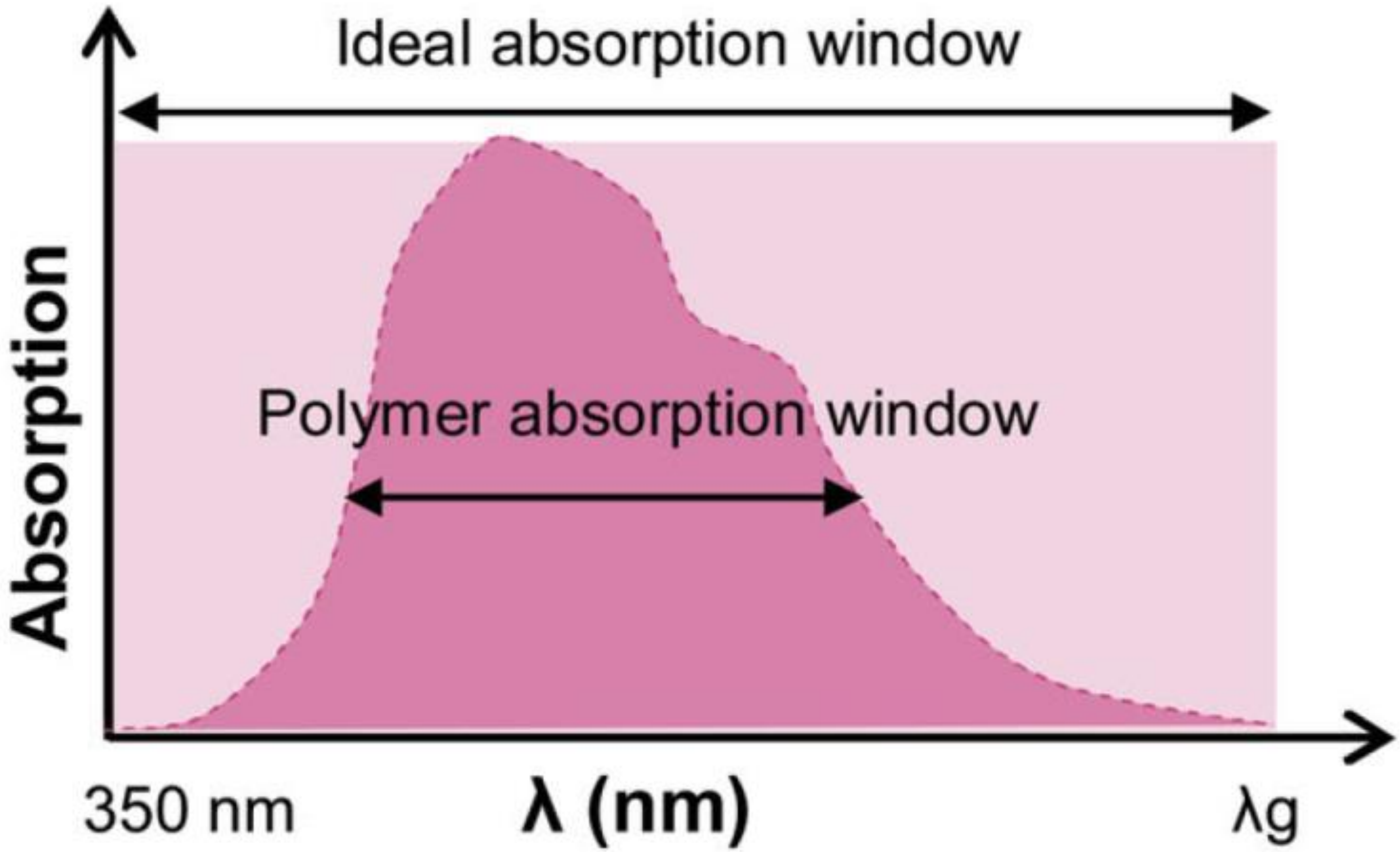

[14]

Ternary blend organic solar cells

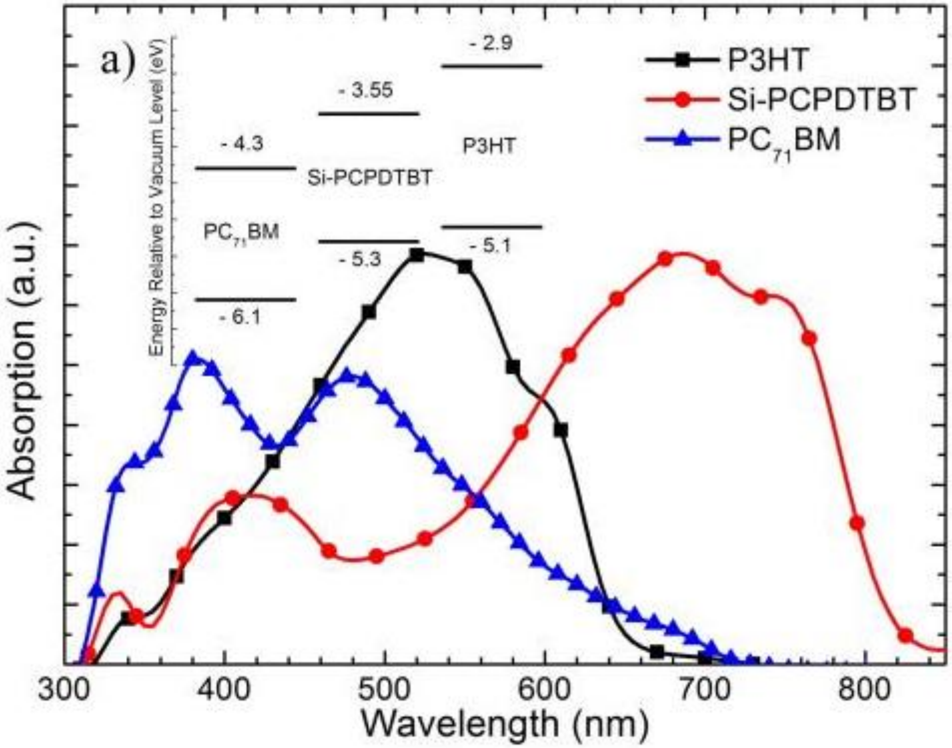

Combine two polymers in the bulk heterojunction active layer

Ratio of P3HT:Si-PCPDTBT set to 7:3

Ternary blend organic solar cells

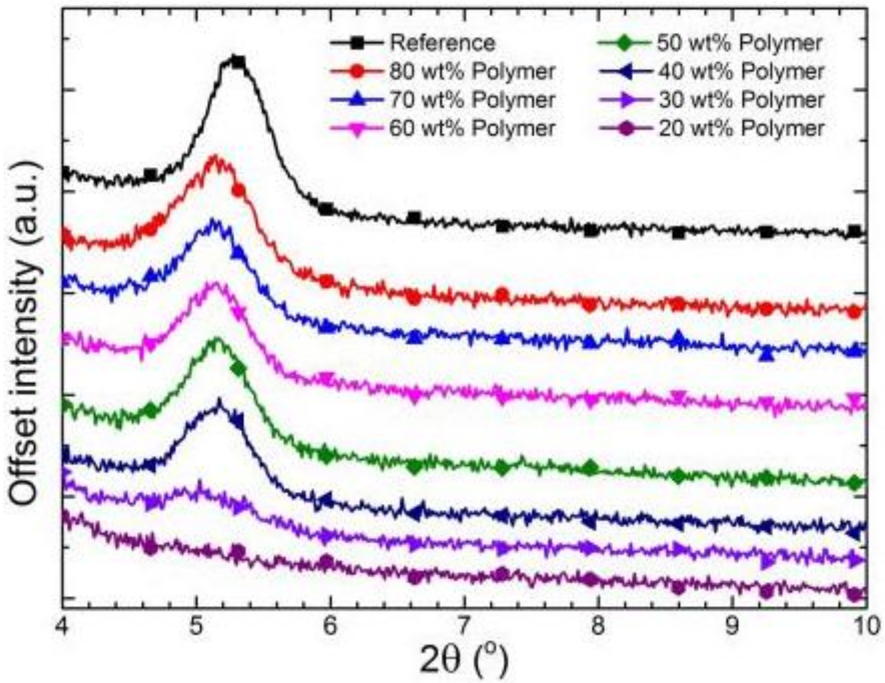

Vary ratio of total polymer (P3HT+Si-PCPDTBT) to $PC_{71}BM$

XRD suggests threshold polymer concentration is required for semi-crystalline film.

Ternary blend organic solar cells

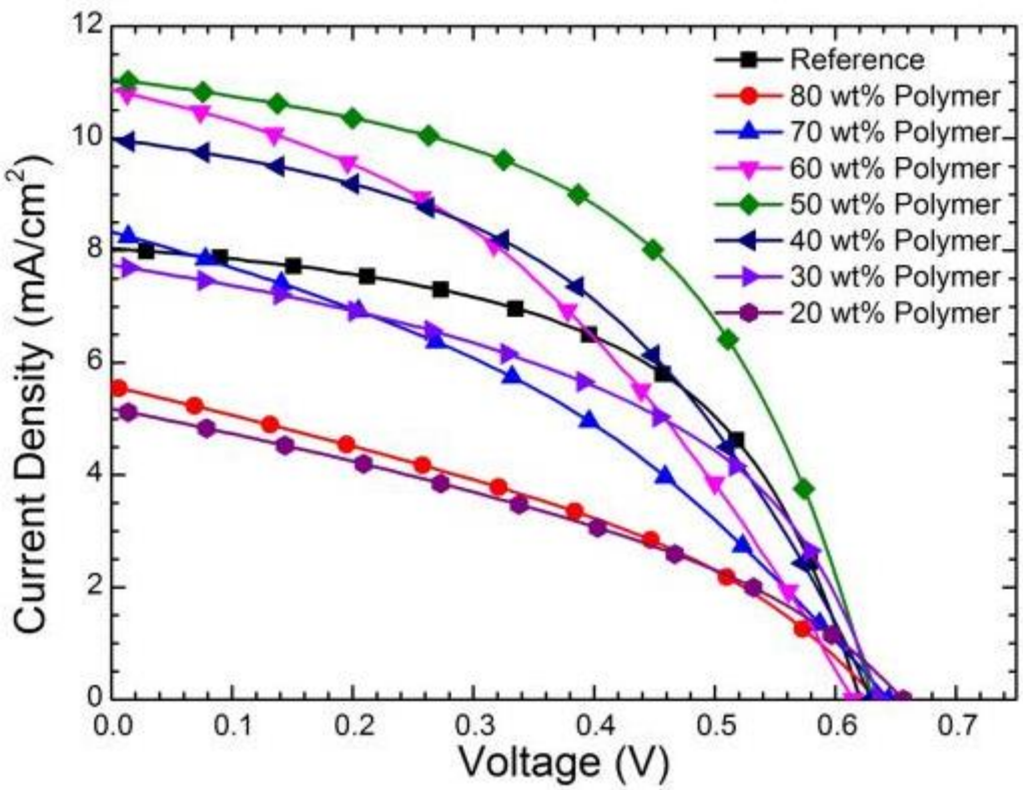

Optimum performance achieved with a balance between polymer and fullerene

Ternary blend organic solar cells

Si-PCPDTBT:PC_{71}BM host system

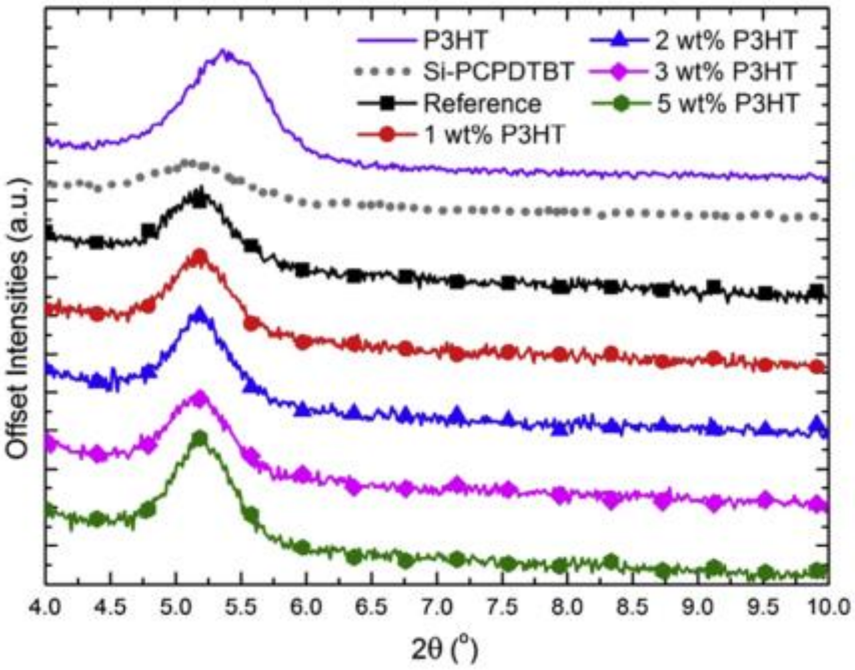

Incorporating small fraction of P3HT caused increase in polymer domain size

[15]

Ternary blend organic solar cells

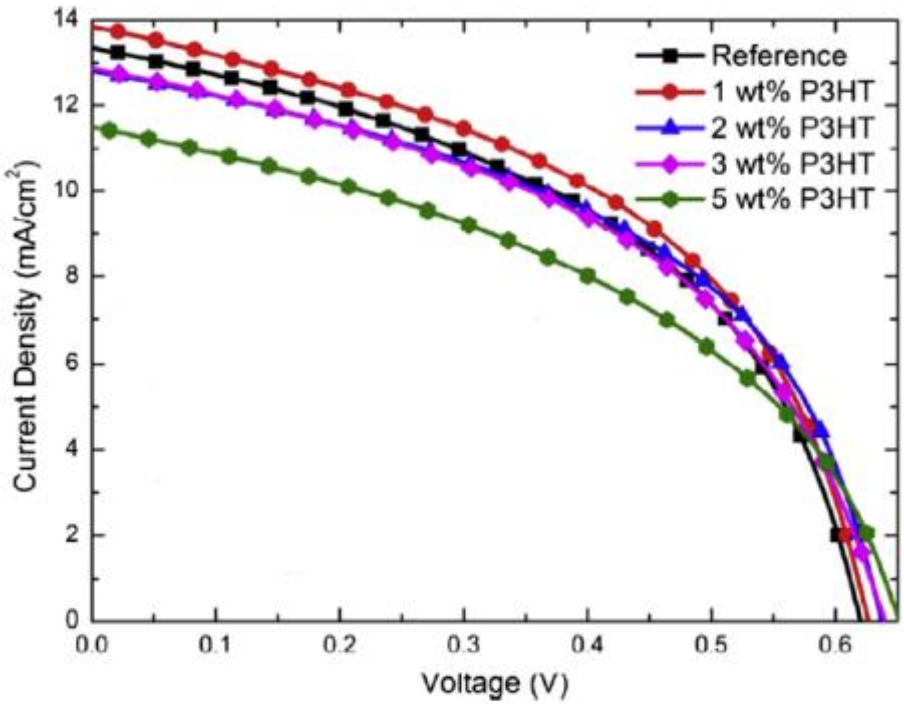

Slight increase in J_{sc}

[15]

Conclusion

- Solution processed roll-to-roll coated OPV devices present multiple unique advantages, including scalability, low embodied energy, and flexibility.
- LCA analysis suggests the embodied energy of OPV modules could be extremely low.
- Multiple demonstration have indicated the viability of solution processed OPV modules.
- Multiple key challenges, such as low efficiency and poor environmental stability, <u>must</u> be addressed before large scale deployment can become a reality.
- Perovskite solar cells may be able to overcome some of these key challenges.

References

[1] J. You, L. Dou, K. Yoshimura, T. Kato, K. Ohya, T. Moriarty, K. Emery, C-C Chen, J. Gao, G. Li, Y. Yang, A polymer tandem solar cell with 10.6% power conversion efficiency, Nature Communications 4 (2013) 1446.

[2] M. Green, K. Emery, Y. Hishikawa, W. Warta, E. Dunlop, Solar cell efficiency tables (Version 45), Progress in Photovoltaics: Research and Applications, 23 (2015) 1-9.

[3] J. H. Yim, S. Joe, C. Pang, K.Mm Lee, H. Jeong,J-Y Park, Y.H. Ahn, J.C. de Mello, S. Lee, Fully solution-processed semitransparent organic solar cells with a silver nanowire cathode and a conducting polymer anode, ACS Nano,8 (2014) 2857-2863.

[4] M.C. Barr, R.M. Howden, R.R Lunt, V. Bulovic, K.K. Gleason, Top-illuminated Organic Photovoltaics on a Variety of Opaque Substrates with Vapour-printed Poly(3,4-ethylenedioxythiophene) Top Electrodes and MoO_3 Buffer Layer, Advanced Energy Materials, 2 (2012) 1404-1409.

[5] N. Espinosa, R.G. Valverde, A. Urbina, F.C. Krebs, A life cycle analysis of polymer solar cell modules prepared using roll-to-roll methods under ambient conditions, Solar Energy Materials and Solar Cells, 95 (2011) 1293-1302.

[6] N. Espinosa, M. Hosel, D. Angmo, F. Krebs, Solar Cells with one-day energy payback for the factories of the future, Energy and Environmental Science, 5 (2012) 5117-5132.

[7] F.C. Krebs, N. Espinosa, M. Hosel, R.R. Sondergard, M. Jorgensen, 25th anniversary article: Rise to power - OPV-based solar parks, Advanced Materials 26 (2014) 29-38.

References

[8] N. Espinosa, M. Hosel, M. Jorgensen, F.C. Krebs, Large scale deployment of polymer solar cells on land, on sea and in the air, Energy and Environmental Science,7 (2014) 855-866.

[9] J. You, Z. Hong, Y.M. Yang, Q. Chen, M. Cai, T-B Song, C-C Chen, S. Lu, Y. Liu, H. Zhou, Y. Yang, Low-Temperature Solution-Processed Perovskite Solar Cell with High Efficiency and Flexibility, ACS Nano, 8 (2014) 1674-1680.

[10] K. Hwang, Y-S Jung, Y-J Heo, F.H. Scholes, S.E. Watkins, J. Subbiah, D.J. Jones, D.Y. Kim, D. Vak, Toward Large Scale Roll-to-Roll Production of Fully Printed Perovskite Solar Cells, DOI: 10.1002/adma.201404598.

[11] M. Jørgensen, K. Norrman, S.A. Gevorgyan, T. Tromholt, B. Andreasen, F.C. Krebs, Stability of Polymer Solar Cells, Advanced Materials, 24 (2012) 580-612.

[12] S. Gevorgyan et al., Interlaboratory outdoor stability studies of flexible roll-to-roll coated organic photovoltaic modules: Stability over 10 000h, Solar Energy Materials and Solar Cells 116 (2013) 187-196.

[13] R. Lin, M. Miwa, M. Wright, Optimisation of the sol-gel derived ZnO buffer layer for inverted structure bulk heterojunction organic solar cells using a low band gap polymer, Thin Solid Films, 566 (2014) 99-107.

[14] T. Ameri, P. Khoram, J. Min, C.J. Brabec, Organic Ternary Solar Cells: A Review, Advanced Materials, 25 (2013) 4245-4266.

[15] R. Lin, M. Wright, K.H. Chan, B. Puthen-Veetil, R. Sheng, X. Wen, A. Uddin, Performance improvement of low band gap polymer bulk heterojunction solar cells by incorporating P3HT, Organic Electronics, 15 (2014) 2837-2846.